



# Plant Archives

Journal homepage: <http://www.plantarchives.org>

DOI Url : <https://doi.org/10.51470/PLANTARCHIVES.2025.v25.no.1.154>

## ANTIFUNGAL EFFICACY OF GREEN-SYNTHEMIZED ZINC OXIDE NANOPARTICLES AGAINST *FUSARIUM* SPP.: AN *IN VITRO* STUDY

Rashmita Saikia<sup>1\*</sup>, Supriya Sharma<sup>1</sup>, Pranjal Kumar Kaman<sup>1</sup> and Arkadeb Chatterjee<sup>2</sup>

<sup>1</sup>Department of Plant Pathology, Faculty of Agriculture, Assam Agricultural University, Jorhat - 785 013, Assam, India

<sup>2</sup>Department of Nematology, Faculty of Agriculture, Assam Agricultural University, Jorhat - 785 013, Assam, India

ORCID identifier: <https://orcid.org/0099-0001-3113-6002> (Rashmita Saikia)

\*Corresponding author E-mail : [elie2045@gmail.com](mailto:elie2045@gmail.com)

(Date of Receiving-12-11-2024; Date of Acceptance-30-01-2025)

### ABSTRACT

Biosynthesis of nanoparticles has received much attention as compared to physical or chemical synthesis due to its eco-friendly nature, low toxicity, production of stable nanoparticles and ease of preparation. In this study, *in vitro* efficacy of green synthesized Zinc oxide nanoparticles (ZnO NPs) has been evaluated against two fungal wilt pathogens viz., *Fusarium oxysporum* f.sp. *cubense* (*Foc*) and *Fusarium oxysporum* f.sp. *lycopersici* (*Fol*). The biological synthesis of ZnO NPs was carried out from two different plant and microbial sources followed by their characterization through UV-Vis spectroscopy, Zeta sizer, FTIR and TEM analysis. Further, these synthesized NPs were tested against the two phytopathogens at three different concentrations (100 ppm, 150 ppm and 200 ppm). Among these, 200 ppm concentration of the synthesized NPs exhibited comparatively more inhibition against the two tested pathogens. Moreover, the treatments with 200 ppm concentration showed highest inhibition against *Foc*. Hence, the results suggest the incorporation of ZnO NPs as an effective antimicrobial agent in agricultural as well as food safety applications.

**Key words :** Characterization, *Fusarium* spp., Green synthesis, *In vitro* efficacy.

### Introduction

Fusarium wilt is a destructive plant disease caused by the soil-dwelling fungus *Fusarium oxysporum*. This disease attacks a wide range of plant species around the world, including important food crops like tomatoes, potatoes, melons, legumes, melons, and bananas. The spores of this pathogen can survive in soil for several years in a dormant state, serving as a great source of inoculum for carrying the disease to next season's crops. The fungus can spread from one place to another through contaminated soil, water, infected seeds and as air-borne spores. *F. oxysporum* enters the plant through the root system and grows into the xylem vessels. It obstructs the vascular system and prevents water and nutrient transport to the plant, eventually resulting in wilting, discoloration and death of the plant (Gupta *et al.*, 2018).

Although, various management strategies viz., cultural, chemical, physical, biological, mechanical, etc. have been in practice to control the pathogen, no effective

management has been achieved yet. Often the fungicides or other chemical compounds which are used to control the different plant diseases have adverse effects on humans, animals as well as environment (Del Puerto Rodríguez *et al.*, 2014). Over time, the continuous use of these chemicals have led to the rise of resistant fungal strains which have been found to acquire resistance by development of mutant genes and become immune to fungicides (Dinham and Malik, 2003). As a result, effective control of phytopathogenic fungus requires the use of environmentally friendly and cost-effective management approaches. One such alternative is the use of nanotechnology, which has emerged as a promising technique for treating several diseases that inhibit plant growth and development. Nanotechnology has been gaining importance in the agricultural sector due to its widespread use in research and application in food industries (Rakibuzzaman *et al.*, 2018) as well as its use in various pesticide and fertilizer industries for the

development of nanopesticides and nanofertilizers (Gogos *et al.*, 2012 and Sturikova *et al.*, 2018).

Biosynthesis of nanoparticles through the use of plant and microbial extract has received much attention as compared to chemical or physical synthesis due to their large surface area, their biocompatibility, low toxicity, and eco-friendly nature of the process and nanoparticles. Methods of chemical synthesis often utilize harmful chemicals, high pressure, energy and temperature. Thus, biological systems serve as a promising tool for synthesis of nanoparticles. The use of fungi for synthesis of nanoparticles offers certain advantages over using other microbes such as bacteria, including scaling up and easy downstream processing, economic feasibility, and greater surface area provided by fungal mycelia (Mukherjee *et al.*, 2001). Fungi require simple nutrients, are easy to handle, have a high wall binding capacity, and have excellent intracellular metal uptake capacities (Kaman and Dutta, 2019). Certain plants (particularly medicinal plants) are also used in the manufacture of nanoparticles because they include natural capping agents such as alkaloids and phenolics, which aid in nanoparticle capping and (Amin *et al.*, 2012).

Highly ionic nanoparticulate metal oxides such as zinc oxide nanoparticles (ZnO NPs) are unique in that they can be produced with high surface areas and with unusual crystal structures (Klabunde *et al.*, 1996). Compared to other organic materials, inorganic materials such as ZnO offer superior durability, greater selectivity, and heat resistance (Padmavathy and Vijayaraghavan, 2008). Moreover, zinc is a mineral element which is considered essential for human health and ZnO can be taken as a form of daily supplement as ZnO NPs have good biocompatibility with human cells (Padmavathy and Vijayaraghavan, 2008). In agriculture, zinc compounds have been used mainly in the form of fungicides. ZnO NPs have considerable advantages over other nanoparticles in terms of their low cost, antimicrobial activity (Kumar *et al.*, 2018a,b; Li *et al.*, 2009) and antifungal activity (Arciniegas-Grijalba *et al.*, 2019; Kairyte *et al.*, 2013) in addition to being an important micronutrient in agriculture (Prasad *et al.*, 2017; Sabir *et al.*, 2014). It is believed that smaller the size of ZnO NPs, stronger the antimicrobial activity projected (Yamamoto, 2001). With the increasing demand and use of nanotechnology, particularly green synthesis of nanoparticles for effective plant disease management, the current work had been designed to synthesize and investigate the antimicrobial activity of green synthesized ZnO NPs against Fusarium wilt pathogens.

## Materials and Methods

### Source of microorganisms and plants for green synthesis of ZnO NPs

The culture of *Trichoderma harzianum* (Accession No. KF439052) was obtained from the culture collection center maintained at the Biocontrol Laboratory, Department of Plant Pathology, Assam Agricultural University, Jorhat, Assam, India. Fresh leaves of *Piper nigrum* were sourced from the All India Coordinated Research Project on Medicinal and Aromatic Plants (AICRP-MAP) plot, located within the horticultural orchard at Assam Agricultural University, Jorhat, Assam, India.

### Biomass production of microbes

Inoculum from culture tubes of *T. harzianum* collected was transferred onto Petri dishes containing Potato Dextrose Agar (PDA) medium, and subsequently inoculated into Potato Dextrose Broth (PDB) medium under aseptic conditions. The cultures were incubated in a B.O.D. incubator at  $26 \pm 1^\circ\text{C}$  for 7 days to facilitate mass cultivation of the microorganism.

### Preparation of plant extract

Fresh, healthy leaves of *P. nigrum* were collected, thoroughly washed with sterile distilled water and then cut into small pieces approximately 5-6 mm in size. The washed plant material was transferred to 150 ml of sterile distilled water and ground using a mechanical mixer grinder. The mixture was then microwaved at 320 MHz for 4 minutes, after which it was allowed to cool to ambient temperature ( $24 \pm 1^\circ\text{C}$ ). The solution was then filtered through Whatman filter paper No. 1 and centrifuged at 10,000 rpm for 15 minutes to further purify the extract. The resulting supernatant was collected and stored at  $4^\circ\text{C}$  for future use. This extract was subsequently utilized for the synthesis of the targeted nanoparticles (Bhuyan *et al.*, 2017).

### Pathogens used in the study

The culture of *Fusarium oxysporum* f.sp. *lycopersici* (*Fol*), the causal agent of Fusarium wilt in tomato, was obtained from the Indian Council of Agricultural Research - National Bureau of Agriculturally Important Microorganisms (ICAR-NBAIM) with ITCC Accession number NAIMCC-F-02784. The culture of *Fusarium oxysporum* f.sp. *cubense* (*Foc*), the causal agent of Fusarium wilt in banana was collected from the culture collection center maintained at the Biocontrol Laboratory, Assam Agricultural University, Jorhat, Assam, India (Accession number SUB11869762 *Foc\_AB07* OP090370). Pure cultures of both the

pathogens were maintained by periodic subculturing onto fresh PDA slants and stored at 4°C for subsequent analysis.

### **Green synthesis of ZnO NPs using plant and microbial extract**

For the green synthesis of ZnO NPs using plant extract, 50 ml of the plant extract earlier prepared was mixed with 50 ml of a 0.1 M zinc nitrate hexahydrate [Zn (NO<sub>3</sub>)<sub>2</sub>·6H<sub>2</sub>O] precursor solution in a 250 ml Erlenmeyer flask. The mixture was then continuously stirred on a magnetic stirrer at 70°C. In a similar approach for the synthesis of ZnO NPs using the biocontrol agent *T. harzianum*, the culture obtained from PDB was harvested and centrifuged at 5000 rpm for 10 minutes at 4°C to collect the supernatant. Subsequently, 50 ml of this microbial supernatant was mixed with 50 ml of the 0.1 M Zn (NO<sub>3</sub>)<sub>2</sub>·6H<sub>2</sub>O precursor solution in a 250 ml Erlenmeyer flask, and the solution was stirred continuously at 70°C. The pH of the mixture was adjusted to 8 by slowly adding 4 M Sodium Hydroxide (NaOH) solution drop by drop until a white precipitate was obtained. The color of the solution changed to a constant yellowish-white, grayish-white, or pure white upon precipitation, indicating the successful formation of ZnO NPs. The precipitate was then extracted by centrifugation at 10,000 rpm for 5-10 minutes, followed by subsequent washing with ethanol and distilled water. Finally, the precipitate was dried overnight at 72-80°C to obtain the ZnO nanoparticle powder, which was stored in airtight vials for further *in vitro* analysis (Zaki *et al.*, 2021).

### **Characterization of biosynthesized ZnO NPs**

The characterization of the synthesized ZnO NPs was conducted using various techniques, including UV-Vis spectrophotometry, Dynamic Light Scattering (DLS) analysis, Zeta Potential analysis, Fourier Transform Infrared Spectroscopy (FTIR), and Transmission Electron Microscopy (TEM) studies. These methods provided detailed insights into the optical properties, particle size distribution, surface charge, chemical composition and morphology of the synthesized nanoparticles.

#### **UV-Vis spectrophotometry analysis**

The formation of ZnO NPs was confirmed through UV-Vis spectrophotometry analysis. The color change observed after exposing the precursor solution to the microbial and plant extract was used as an indicator of ZnO NPs formation. This color change is attributed to the Surface Plasmon Resonance (SPR) phenomenon, which occurs due to the interaction of the nanoparticles with light, confirming the synthesis of ZnO NPs.

#### **Dynamic Light Scattering (DLS) analysis**

DLS was employed to determine the average particle size of the biosynthesized ZnO NPs. Prior to analysis, the sample was prepared by dispersing a small amount of ZnO NPs powder in a suitable solvent (organic solvent like ethanol or deionized water) followed by adding a stabilizing agent to prevent aggregation (SDS or CTAB). Then the sample was sonicated three to four times to ensure uniform dispersion. The particle size distribution was then measured using a computer-controlled particle size analyzer (ZETA sizer, Nanoseries, Malvern Instrument Nano Zs, 2000). This method provided detailed information about the size distribution and homogeneity of the nanoparticles in the sample.

#### **Zeta Potential**

Zeta potential is an essential parameter for assessing the surface charge of nanoparticles and predicting their long-term stability. For the zeta potential measurement, 2 ml of the prepared sample was transferred into a cuvette. The surface charge and particle distribution in the liquid were then analyzed using a computer-controlled charge analyzer (Zetasizer Nano ZS, Malvern Instruments Ltd.), providing insights into the stability and dispersibility of the nanoparticles.

#### **Fourier Transform Infrared Spectrometer (FTIR)**

The FTIR spectra of the biosynthesized ZnO NPs was recorded to determine whether the functional groups associated with reductive biomolecules exist and to identify the groups involved in the reduction of ZnO into nanoparticles. The infrared (IR) spectra were obtained using a Fourier Transform Infrared Spectrometer (Shimadzu, Japan), scanning the spectral range between 400 and 4000 cm<sup>-1</sup>. The spectra were averaged from 50 scans, recorded at a resolution of 4 cm<sup>-1</sup>.

#### **Transmission Electron microscope (TEM)**

TEM is a valuable technique for evaluating the size and morphology of synthesized nanoparticles. TEM analysis was performed at the Central Instrumentation Facility (CIF) at the Indian Institute of Technology (IIT), Guwahati, Assam, India using a 200 kV Field Transmission Electron Microscope with Energy Dispersive X-ray Spectroscopy (EDS) (JEM-100F). The analysis was conducted at a voltage of 20 kV and a magnification of 20,000X, allowing for detailed characterization of the ZnO nanoparticle's size, shape, and elemental composition.

#### ***In vitro* study of ZnO NPs against the pathogens**

An *in vitro* assay was conducted to evaluate the antifungal efficacy of green-synthesized ZnO NPs against *Foc* and *Fol* using the Poisoned Food Technique (Kim *et*

*al.*, 2012). The antifungal activity of the ZnO NPs was tested at three different concentrations (100, 150 and 200 ppm), and the results were compared with a chemical control (Amistar® 1%) and an untreated control.

To prepare the treatments, different concentrations of ZnO NPs were incorporated into a series of 100 ml of lukewarm molten PDA. The mixture was poured into 9 cm Petri plates at a rate of 20 ml poisoned media per plate and allowed to solidify. Fungal mycelium (5 mm diameter) was excised from the periphery of 7-10 days old actively growing cultures using a sterilized cork borer and placed at the center of the Petri plates. The plates were then incubated at  $27\pm 1^\circ\text{C}$  in a R.E.I.C.O. B.O.D. incubator until full fungal growth was observed in the respective control plates (Kim *et al.* 2012). Each treatment was replicated five times and arranged in a Completely Randomized Design (CRD) to ensure statistical validity. Mycelial growth inhibition over control was calculated for each treatment by Vincent's (1947) formula.

### Statistical analysis

A Completely Randomized Design (CRD) was used for the statistical analysis of the data. The collected data were subjected to statistical analysis using Fisher's method of Analysis of Variance (ANOVA). The significance of variance among the treatments was determined by calculating the "F" value and comparing it with the tabulated "F" value at the 5% level of probability. The percentage values of growth inhibition were converted after Gomez and Gomez (1984) and transformed by angular transformation. Further, the treatments were compared amongst themselves by calculating the critical difference (CD) as follows:

C.D. at 5% = S. Ed  $\times$  't' 5% (error degrees of freedom)

where, the standard error of differences (S.Ed.) of mean was calculated by using the formula:

$$S.Ed(\pm) = \sqrt{\frac{2 \times \text{Error Mean Square}}{\text{No. of replication for each treatment}}}$$

where, S. Ed. = Standard error of difference.

't' 5% = "t critical" for error degree of freedom at 5% level of probability

The significance and non-significance of the treatments at 5% probability level were calculated out by multiplying the S.Ed. with appropriate tabulated value for error degrees of freedom.

## Results and Discussion

### Green synthesis of ZnO NPs

In this study, ZnO NPs were synthesized through a green approach using *P. nigrum* and *T. harzianum*. On addition of NaOH to the precursor solution, a turbid white color solution was obtained. This solution was further processed till it was converted to white powdery precipitate which confirmed the formation of ZnO NPs (Fig. 1). The formation of ZnO NPs is due to the phytochemicals present in the plant or microbial extract which act as reducing agents for converting the metal precursors to metal nanoparticles. Phytochemicals such as terpenoids, flavonoids, phenolic compounds, aldehydes and alkaloids are considered to be antioxidants and toxic-free chemicals which can act as both reducing and stabilizing agents. Therefore, the extract composition has a significant effect on nanoparticle synthesis (Jayachandran *et al.*, 2021).



Fig. 1 : Green synthesized ZnO NPs.

### Characterization of ZnO NPs

#### UV-Vis spectrophotometry analysis

The formation of ZnO NPs was further confirmed by UV-Vis spectrophotometry analysis which showed the formation of characteristic SPR bands at 356 nm (*P.*

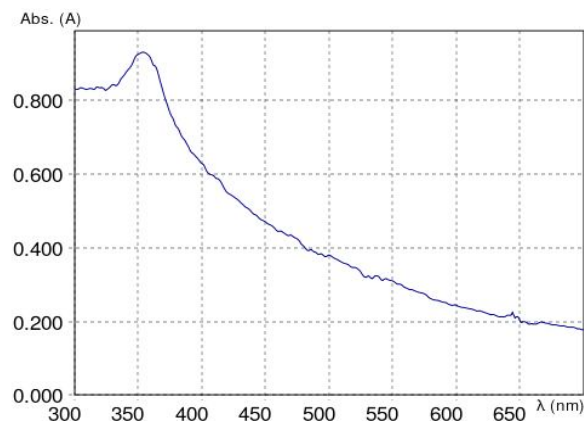
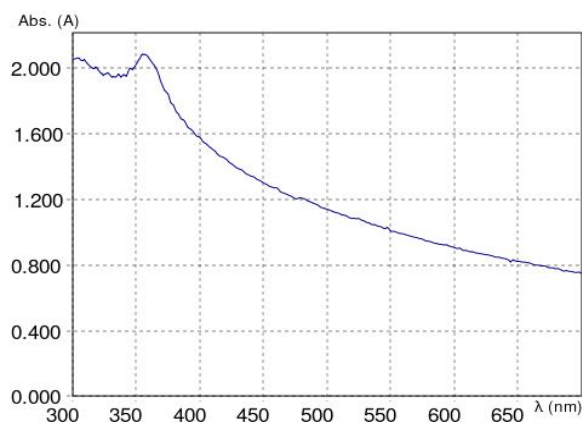
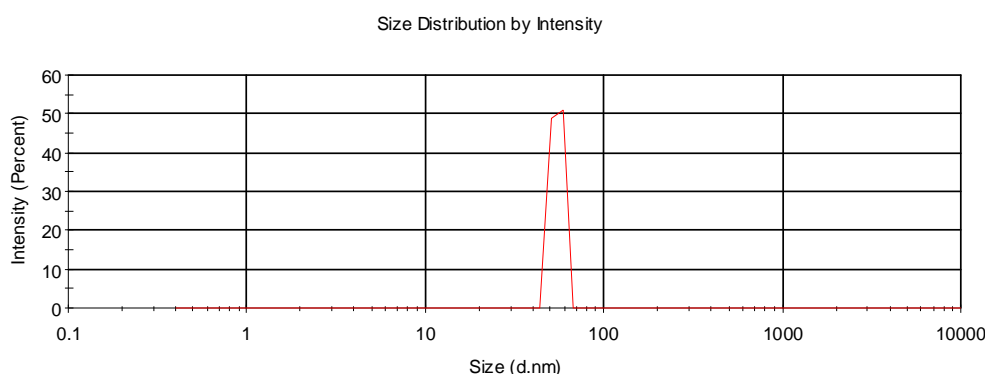


Fig. 2a : UV-Vis absorption spectra for ZnO NPs obtained from *P. nigrum*.



**Fig. 2b** : UV-Vis absorption spectra for ZnO NPs obtained from *T. harzianum*.

ZnO NPs synthesized from *P. nigrum* was 54.85 nm with a Poly Dispersity Index (PDI) of 0.994 and the size obtained for ZnO NPs synthesized from *T. harzianum* was 68.06 nm with a PDI of 0.247 (Figs. 3a & 3b). Hence, we can say that since the value of PDI is larger than 0.10, the biosynthesized nanoparticles are polydispersed in nature (Hughes *et al.*, 2015). Similar findings were recorded by Gupta *et al.* (2018) on studying the effective antimicrobial activity of green ZnO NPs of *Catharanthus roseus* where they recorded the average size distribution of ZnO NPs in the range of 50.73 nm along with a polydispersity index of 0.780.



**Fig. 3a** : DLS pattern of ZnO NPs synthesized using *P. nigrum*.

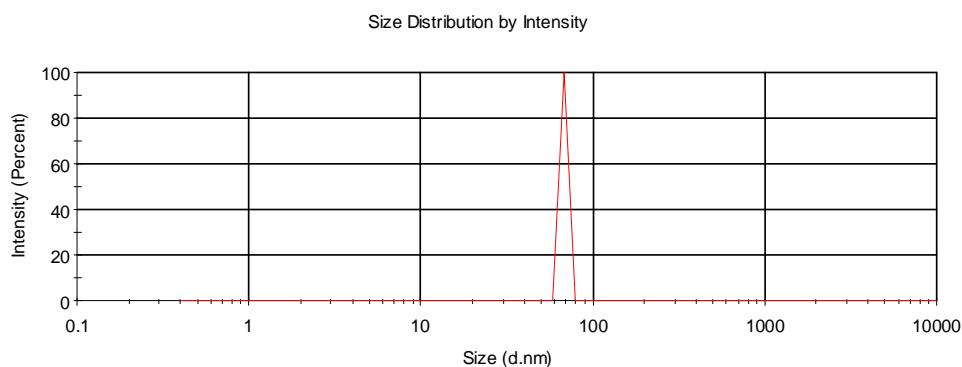


**Fig. 3b** : DLS pattern of ZnO NPs synthesized using *T. harzianum*.

*nigrum* and *T. harzianum*) which are specific for ZnO nanoparticles (Figs. 2a & 2b). This was in accordance to the findings of Zaki *et al.*, (2021) where a peak of 300 nm was obtained for *T. harzianum* mediated ZnO nanoparticles which were used for controlling soil-borne pathogens in cotton. It has been reported that for ZnO nanoparticles, the absorbance peak is usually observed between 310 nm and 360 nm of wavelength (Ghamsari *et al.*, 2017).

#### Dynamic Light Scattering (DLS) analysis

DLS analysis revealed that the average size of the

#### Zeta Potential

Zeta potential analysis showed that biosynthesized ZnO NPs from *P. nigrum* and *T. harzianum* were negatively charged with zeta potential of -3.01 mV and -9.57 mV, respectively (Figs. 4a & 4b) Similarly, Chaudhuri and Malodia (2017) reported negative zeta potential (-20.7 mV) of ZnO NPs and mentioned that negative value results in repulsion among the particles thus stabilizing the NPs. Thus, results depicted that synthesized ZnO NPs are stable in nature and have less chances of agglomeration. The results of the present study are also

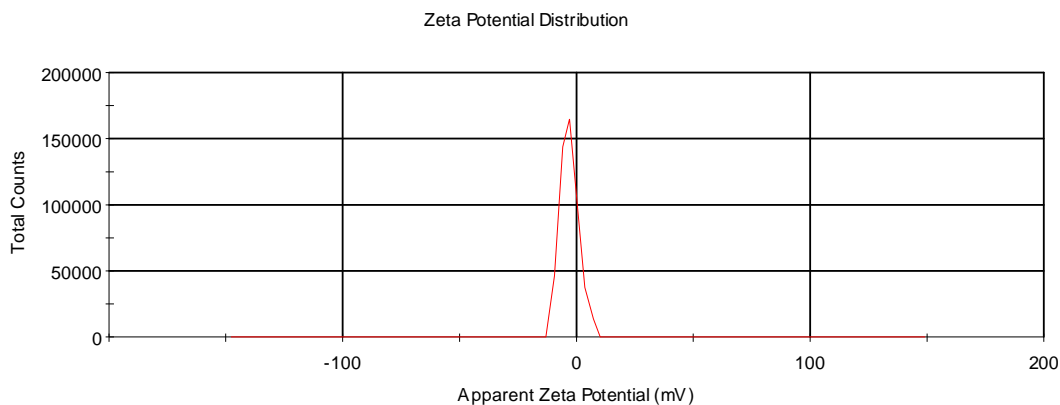


**Fig. 4a :** Zeta potential of ZnO NPs synthesized using *P. nigrum*.

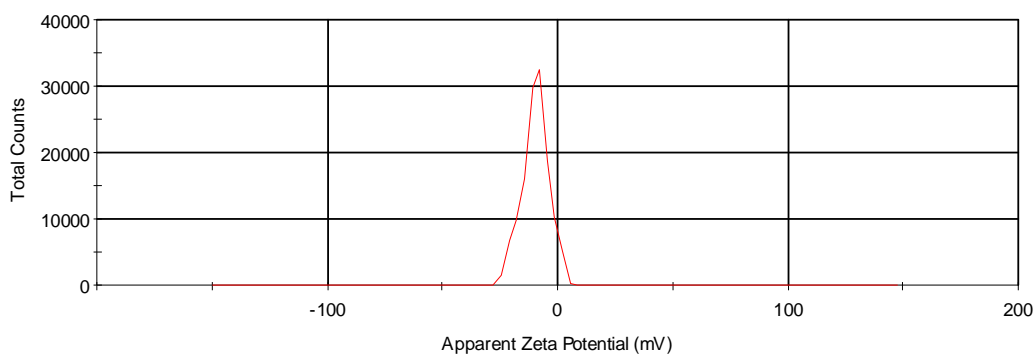


**Fig. 4b :** Zeta potential of ZnO NPs synthesized using *T. harzianum*.

in agreement with the study of Nallamuthu (2015), who reported that zeta potential of  $\pm 30$  is ideal for any suspension and considered as stable in nature with very low affinity for agglomeration. The Zeta potential measurements thus verify and support the dispersion capacity of the green synthesized ZnO NPs. The negative surface charge is due to the binding affinity of extract compounds with the NPs, conferring stability to the ZnO NPs and alleviating the aggregation potential of the particles.

#### Fourier Transformed Infrared Spectrometer (FTIR)

FTIR spectra of the nanoparticles were recorded to figure out if the functional groups related to these reductive biomolecules exists and specifying the functional groups that contributed to the reduction of the ZnO into nanoparticles. The spectral peaks observed for ZnO NPs synthesized from both *P. nigrum* and *T. harzianum* were at 2981.9, 2890.6, 1382.8, 1250.5, 1151.7, 1071.6, 3652.8, 1382.8, 1252.4, 1149.9, 1079.1, 1026.9, 713.8, 954.2 and 844.2 (Fig. 5a & 5b) revealing the presence of functional groups such as C-H (alkane), C=O (carboxylic acid), C-O (Primary alcohol), Ester carbonyl, C-O (Ether). Similarly, Munis *et al.*, (2022) conducted FTIR

spectroscopy for ZnO NPs synthesized from *T. harzianum* which displayed the presence of reducing and stabilizing chemical compounds such as alcohol, carboxylic acid, amines, and alkyl halide. Moreover, Barzinjy and Azeez (2020) recorded FTIR spectra on characterization of ZnO NPs synthesized using *Eucalyptus globulus* Labill. leaf extract where the band at  $1363\text{ cm}^{-1}$  correlated to the C-O stretching of the carboxylic acid group, while the band found at  $1483\text{ cm}^{-1}$ , most probably, related to the -C=C- stretching of the aromatic compounds. The robust and relatively wide band at  $3430\text{ cm}^{-1}$  could be allocated to the O-H stretching of phenolic compounds.

#### Transmission Electron Microscopy (TEM)

Study on shape and nature of synthesized ZnO NPs was done by TEM and results showed irregularly spherical shaped ZnO NPs with a size ranging from 17 to 99 nm and Selected Area Electron Diffraction (SAED) pattern showed that they were crystalline in nature (Fig. 6a & 6b). Similar findings were recorded by Zaki *et al.*, (2021), where the TEM analysis of the ZnO NPs synthesized from *T. harzianum* showed a mixture of hexagonal, spherical and rod-shaped small particles and crystalline



**Table 1 :** *In vitro* efficacy of green synthesized ZnO NPs against *Foc* and *Fol* at 100, 150 and 200 ppm concentrations.

Treatments	Mycelial growth* (cm)	Percent inhibition over control
T <sub>1</sub> : ZnO NP ( <i>P. nigrum</i> ) @100ppm+ <i>Foc</i>	7.20 <sup>e</sup>	20.00
T <sub>2</sub> : ZnO NP ( <i>P. nigrum</i> ) @150ppm+ <i>Foc</i>	5.60	37.77
T <sub>3</sub> : ZnO NP ( <i>P. nigrum</i> ) @200ppm+ <i>Foc</i>	3.70 <sup>b</sup>	58.88
T <sub>4</sub> : ZnO NP ( <i>P. nigrum</i> ) @100ppm+ <i>Fol</i>	8.00 <sup>c</sup>	11.11
T <sub>5</sub> : ZnO NP ( <i>P. nigrum</i> ) @150ppm+ <i>Fol</i>	7.00	22.22
T <sub>6</sub> : ZnO NP ( <i>P. nigrum</i> ) @200ppm+ <i>Fol</i>	6.50 <sup>d</sup>	27.77
T <sub>7</sub> : ZnO NP ( <i>T. harzianum</i> ) @100ppm+ <i>Foc</i>	7.30 <sup>e</sup>	18.88
T <sub>8</sub> : ZnO NP ( <i>T. harzianum</i> ) @150ppm+ <i>Foc</i>	4.80	46.66
T <sub>9</sub> : ZnO NP ( <i>T. harzianum</i> ) @200ppm+ <i>Foc</i>	3.50 <sup>b</sup>	61.11
T <sub>10</sub> : ZnO NP ( <i>T. harzianum</i> ) @100ppm + <i>Fol</i>	8.00 <sup>c</sup>	11.11
T <sub>11</sub> : ZnO NP ( <i>T. harzianum</i> ) @150ppm + <i>Fol</i>	6.60 <sup>d</sup>	26.66
T <sub>12</sub> : ZnO NP ( <i>T. harzianum</i> ) @200ppm + <i>Fol</i>	5.20	42.22
T <sub>13</sub> : Chemical control ( <i>Foc</i> )	1.80 <sup>a</sup>	80.00
T <sub>14</sub> : Chemical control ( <i>Fol</i> )	2.00 <sup>a</sup>	77.77
T <sub>15</sub> : Untreated Control	9.00	0.00
S.Ed. (±)	0.47	
CD <sub>(0.05)</sub>	0.88	

\*Data are mean of five replications

\*Data followed by same alphabets are statistically at par.

synthesized from *T. harzianum* followed by 200 ppm concentration of ZnO NPs synthesized from *P. nigrum* which resulted in 58.88% inhibition against *Foc*. Chemical control showed maximum mycelial inhibition of 78.22%. Similar findings were recorded by Munis *et al.* (2022) who investigated the efficacy of mycosynthesized ZnO NPs from *T. harzianum* against fusarium wilt of chickpea and recorded maximum inhibition of 85.2% at 0.50 µg/ml concentration of ZnO NPs followed by 75.1% inhibition at a concentration of 0.25 µg/ml. The higher efficacy of ZnO NPs at 200 ppm observed in the present study is due to the smaller size of ZnO NPs which help in rapid accumulation on the fungal mycelium and then penetration inside it (Stroz and Imlay, 1999). Additionally, Hwang *et al.*, (2008) reported that nanoparticle on entering inside the fungal mycelium causes interruption in the metabolic

processes and respiration by reaction with cellular molecules. Exposure to ZnO NPs also decreases the content of non-enzymatic glutathione (GSH) concentration inside the fungal cells (Suman and Kirubakaran, 2015). GSH has been reported to modulate cellular processes like stabilization of cell membrane (Meister, 1983), regulation of gene expression and apoptosis (Grosicka, 2005). Thus, decrease in GSH level disturbs the normal cellular processes thereby making the fungal cells more vulnerable to oxidative damage. Results also revealed that the effect the efficacy was more pronounced for ZnO NPs synthesized from microbes as compared to those synthesized from plants. It has been found that microorganisms have the ability to accumulate and detoxify heavy metals due to various reductase enzymes, which are able to reduce metal salts to metal nanoparticles with a narrow size distribution and, therefore, less polydispersity (Singh *et al.*, 2016). Moreover, compared with bacteria, fungi have higher tolerances to, and uptake competences for, metals, particularly in terms of the high wall-binding capability of metal salts with fungal biomass for the high-yield production of nanoparticles (Alghuthaymi *et al.*, 2015; Castro-Longoria *et al.*, 2011).

### Acknowledgement

The authors extend their gratitude towards Biocontrol Laboratory, Department of Plant Pathology, Assam Agricultural University, Jorhat, Assam, India and National Bureau of Agriculturally Important Microorganisms (NBAIM), Mau, Uttar Pradesh, India for providing the microbial cultures needed to carry out the experiment and the Directorate of Post Graduate Studies, Assam Agricultural University, Assam, India for providing all the necessary facilities during the entire course of investigation.

### References

- Alghuthaymi, M.A., Almoammar H., Rai M., Said-Galiev E. and Abd-Elsalam K.A. (2015). Myconanoparticles: synthesis and their role in phytopathogens management. *Biotechnol. Biotechnol. Equip.*, **29**, 221-236.
- Amin, M., Anwar F., Janjua A., Iqbal M.A. and Rashid U. (2012). Green synthesis of silver nanoparticles through reduction with *Solanum xanthocarpum* L. berry extract: characterization, antimicrobial and urease inhibitory activities against *Helicobacter pylori*. *Int. J. Mol. Sci.*, **13**, 9923-9941.
- Arciniegas-Grijalba, P.A., Patiño-Portela M.C., Mosquera-

- Sánchez L.P., Sierra B.G., Muñoz-Florez J.E., Erazo-Castillo L.A. and Rodríguez-Páez J.E. (2019). ZnO-based nanofungicides: Synthesis, characterization and their effect on the coffee fungi *Mycena citricolor* and *Colletotrichum* sp. *Mater. Sci. Eng: C*, **98**, 808-825.
- Barzinjy, A.A. and Azeez H.H. (2020). Green synthesis and characterization of zinc oxide nanoparticles using *Eucalyptus globulus* Labill. leaf extract and zinc nitrate hexahydrate salt. *SN Appl. Sci.*, **2**, 99.
- Bhuyan, B., Paul A., Paul B., Dhar S.S. and Dutta P. (2017). *Paederia foetida* Linn. promoted biogenic gold and silver nanoparticles: synthesis, characterization, photocatalytic and *in vitro* efficacy against clinically isolated pathogens. *J. Photochem. Photobiol. B*, **173**, 210-215.
- Castro-Longoria, E., Vilchis-Nestor A.R. and Avalos-Borja M. (2011). Biosynthesis of silver, gold and bimetallic nanoparticles using the filamentous fungus *Neurospora crassa*. *Colloids Surf B Biointerfaces*, **83**, 42-48.
- Chaudhuri, S.K. and Malodia L. (2017). Biosynthesis of zinc oxide nanoparticles using leaf extract of *Calotropis gigantea*: characterization and its evaluation on tree seedling growth in nursery stage. *Appl. Nanosci.*, **7**, 501-512.
- del Puerto Rodríguez, A.M., Tamayo S.S. and Estrada D.E.P. (2014). Effects of pesticides on health and the environment. *Rev Cuba de Hig y Epidemiologia*, **52**, 372-387.
- Dinham, B. and Malik S. (2003). Pesticides and human rights. *Int. J. Occup. Environ. Health*, **9**, 40-52.
- Grosicka, E., Sadurska B., Szumiło M., Grzela T., Łazarczyk P., Niderla-Bielińska J. and Rahden-Staroń I. (2005). Effect of glutathione depletion on apoptosis induced by thiram in Chinese hamster fibroblasts. *Int. Immunopharmacol.*, **5**, 1945-1956.
- Gogos, A., Knauer K. and Bucheli T.D. (2012). Nanomaterials in plant protection and fertilization: current state, foreseen applications and research priorities. *J. Agric. Food Chem.*, **60**, 9781-9792.
- Gomez, K.A. and Gomez A.A. (1984). *Statistical procedures for agricultural research*. John Wiley & Sons.
- Gupta, M., Tomar R.S., Kaushik S., Mishra R.K. and Sharma D. (2018). Effective antimicrobial activity of green ZnO nanoparticles of *Catharanthus roseus*. *Front. Microbiol.*, **9**, 2030.
- Hughes, J.M., Budd P.M., Grieve A., Dutta P., Tiede K. and Lewis J. (2015). Highly monodisperse, lanthanide containing polystyrene nanoparticles as potential standard reference materials for environmental “nano” fate analysis. *J. Appl. Polym. Sci.*, **132**.
- Hwang, E.T., Lee J.H., Chae Y.J., Kim Y.S., Kim B.C., Sang B.I. and Gu M.B. (2008). Analysis of the toxic mode of action of silver nanoparticles using stress specific bioluminescent bacteria. *Small*, **4**, 746-750.
- Jayachandran, A., Aswathy T.R. and Nair A.S. (2021). Green synthesis and characterization of zinc oxide nanoparticles using *Cayratia pedata* leaf extract. *Biochem. Biophys. Rep.*, **26**, 100995.
- Kairyte, K., Kadys A. and Luksiene Z. (2013). Antibacterial and antifungal activity of photoactivated ZnO nanoparticles in suspension. *J Photochem Photobiol B: Biol.*, **128**, 78-84.
- Kaman, P.K. and Dutta P. (2019). Synthesis, characterization and antifungal activity of biosynthesized silver nanoparticle. *Indian Phytopathol.*, **72**, 79-88.
- Kim, S.W., Jung J.H., Lamsal K., Kim Y.S., Min J.S. and Lee Y.S. (2012). Antifungal effects of silver nanoparticles (AgNPs) against various plant pathogenic fungi. *Mycobiol.*, **40**, 53-58.
- Klabunde, K.J., Stark J., Koper O., Mohs C., Park D.G., Decker S., Jiang Y., Lagadic I. and Zhang D. (1996). Nanocrystals as stoichiometric reagents with unique surface chemistry. *J. Phys. Chem.*, **100**, 12142-12153.
- Kumar, K., Shyamal B.R.K., Gupta A., Mathur M., Swami A.K. and Chaudhary S. (2018a). Efficacious fungicidal potential of composite derived from nano-aggregates of Cu-Diclofenac complexes and ZnO nanoparticles. *Compos. Commun.*, **10**, 81-88.
- Kumar, P., Burman U. and Kaul R.K. (2018b). Ecological risks of nanoparticles: effect on soil microorganisms. In: *Nanomaterials in Plants, Algae and Microorganisms* (pp. 429-452). Academic Press.
- Li, X., Xing Y., Jiang Y., Ding Y. and Li W. (2009). Antimicrobial activities of ZnO powder coated PVC film to inactivate food pathogens. *Int. J. Food Sci. Technol.*, **44**, 2161-2168.
- Meister, A. (1983) Selective modification of glutathione metabolism. *Science*, **220**, 472-477.
- Mukherjee, P., Ahmad A., Mandal D., Senapati S., Sainkar S.R., Khan M.I., Parishcha R., Ajaykumar P.V., Alam M., Kumar R. and Sastry M. (2001). Fungus-mediated synthesis of silver nanoparticles and their immobilization in the mycelial matrix: a novel biological approach to nanoparticle synthesis. *Nano lett.*, **1**, 515-519.
- Munis, M.F.H., Alamer K.H., Althobaiti A.T., Kamal A., Liaquat F., Haroon U., Ahmed J., Chaudhary H.J. and Attia H. (2022). ZnO Nanoparticle-Mediated Seed Priming induces Biochemical and Antioxidant changes in Chickpea to Alleviate Fusarium wilt. *J. Fungi*, **8**, 753.
- Nallamuthu, I., Devi A. and Khanum F. (2015). Chlorogenic acid loaded chitosan nanoparticles with sustained release property, retained antioxidant activity and enhanced bioavailability. *Asian J. Pharm. Sci.*, **10**, 203-211.
- Padmavathy, N. and Vijayaraghavan R. (2008). Enhanced bioactivity of ZnO nanoparticles—an antimicrobial study. *Sci. Technol. Adv. Mater.*, **9**, 035004.
- Prasad, R., Bhattacharyya A. and Nguyen Q.D. (2017). Nanotechnology in sustainable agriculture: recent developments, challenges and perspectives. *Front. Microbiol.*, **8**, 1014.
- Rakibuzzaman, M., Rahul S.K., Ifaz M.I., Gani O. and Uddin A.F.M.J. (2018). Nano technology in agriculture . Future

- aspects in Bangladesh. *Int. J. Bus. Soc. Sci. Res.*, **7**, 06-09.
- Sabir, S., Arshad M. and Chaudhari S.K. (2014). Zinc oxide nanoparticles for revolutionizing agriculture: Synthesis and applications. *Sci. World J.*, 925494.
- Singh, P., Kim Y.J., Zhang D. and Yang D.C. (2016). Biological synthesis of nanoparticles from plants and microorganisms. *Trends Biotechnol.*, **34**, 588-599.
- Storz, G and Imlay J.A. (1999). Oxidative stress. *Curr. Opin. Microbiol.*, **2**, 188-194.
- Sturikova, H., Krystofova O., Huska D. and Adam V. (2018). Zinc, zinc nanoparticles and plants. *J. Hazard. Mater.*, **349**, 101-110.
- Suman, T.Y., Rajasree S.R. and Kirubakaran R. (2015). Evaluation of zinc oxide nanoparticles toxicity on marine algae *Chlorella vulgaris* through flow cytometric, cytotoxicity and oxidative stress analysis. *Ecotoxicol. Environ. Saf.*, **113**, 23-30.
- Vincent, J.M. (1947). Distortion of fungal hyphae in the presence of certain inhibitors. *Nature*, **159**, 850-850.
- Yamamoto, O. (2001). Influence of particle size on the antibacterial activity of zinc oxide. *Int. J. Inorg. Mater.*, **3**, 643-646.